Processing of CP-Ti by high-pressure torsion and the effect of surface modification using a post-HPT laser treatment

Hsuan-Kai Lin [a], [**], Guan Yuan Li [a], Sarah Mortier [b], [c], Piotr Bazarnik [d], Yi Huang [e], [f], [*], Malgorzata Lewandowska [d], Terence G. Langdon [f]

[a] Graduate Institute of Materials Engineering, National Pingtung University of Science and Technology, Pingtung 912, Taiwan
[b] Ecole Polytechnique Universitaire de Montpellier, 34095 Montpellier CEDEX 5, France
[c] Alten Nantes, 275 Boulevard Marcel Paul, 44800 Saint-Herblain, France
[d] Faculty of Materials Science, Warsaw University of Technology, Woloska 141, 02-507 Warsaw, Poland
[e] Department of Design and Engineering, Faculty of Science and Technology, Bournemouth University, Poole, Dorset BH12 5BB, UK
[f] Materials Research Group, Department of Mechanical Engineering, University of Southampton, Southampton SO17 1BJ, UK

ARTICLE INFO

ABSTRACT

Commercial purity titanium (CP-Ti) was processed by high-pressure torsion (HPT) with various numbers of turns ($N = 1$, 10 and 20). The hardness of the CP-Ti increased with an increasing number of HPT turns due to grain refinement. Tensile testing showed that the HPT-processed 10 turns sample had low ductility and high strength but the ductility may be improved through post-HPT short-term annealing at carefully selected temperatures. Some HPT-processed samples were laser surface-treated with different laser powers and scanning speeds. The surface roughness of the laser-textured samples increased with increasing laser power and led to a lower contact angle which signifies an increased hydrophilicity. After a holding time of 13 days, the samples underwent a hydrophilic-to-hydrophobic transformation as the contact angle increased to as much as 129°. It is concluded that laser surface texture processes are capable of controlling the hydrophilic/hydrophobic properties of ultra-fine grained CP-Ti.

© 2019 Elsevier B.V. All rights reserved.

1. Introduction

Commercial purity titanium (CP-Ti) is one of the most commonly used materials for biomedical applications and implant components due to its good biocompatibility, high fatigue strength, excellent corrosion resistance and non-toxicity [1—3]. However, the mechanical strength of CP-Ti is lower than for titanium alloys, such as the Ti-6Al-4V alloy, and therefore it is often subjected to thermo-mechanical processing to improve its mechanical properties. Studies have shown that the high hydrostatic pressure produced from severe plastic deformation (SPD) is beneficial in refining the grain structure and enhancing the mechanical strength and toughness of engineering metals and alloys [4]. Equal-channel angular pressing (ECAP) [5] and high-pressure torsion (HPT) [4] are particularly effective for achieving ultrafine-grain structures [6—8]. However, for CP-Ti and Ti alloys, the ECAP processing is normally conducted at a high temperature [9] whereas HPT processing can be carried out at room temperature [10]. As a result, the use of HPT is generally preferred for achieving grain refinement and strength enhancement.

The surface characteristics of bulk materials have a significant impact on their performance in power plants, electronics and biomedical applications [11]. Superhydrophobic surfaces have many desirable interface behaviors, including self-cleaning, anti-fouling and anti-attrition. As a result, they are commonly employed in applications such as surgical tools and bio-medical devices [12]. Various researchers have drawn an analogy between the super-hydrophobic metallic surfaces and lotus leaves which are characterised by a dual-scale roughness structure and nanometer scale hairs which trap air between the water droplets and the surface [13—15]. Hydrophilic phenomena provide a good adhesion strength between the matrix and other media and are often exploited as biosensors for cell-cell communications [15,16]. For example, bone

* Corresponding author. Department of Design and Engineering, Faculty of Science and Technology, Bournemouth University, Poole, Dorset BH12 5BB, UK.
** Corresponding author. Graduate Institute of Materials Engineering, National Pingtung University of Science and Technology, Pingtung 912, Taiwan.
E-mail addresses: hklin@mail.npust.edu.tw (H.-K. Lin), yhuang2@bournemouth.ac.uk (Y. Huang).

implants made of titanium alloy must be treated in some ways, such as by sandblasting or acid etching and anodizing, so as to become bioactive and thereby improve their connectivity with the surrounding tissue [17–19]. This means that it is essential to develop an understanding of the basic surface properties of engineering metals and alloys and to devise techniques to modify and control these fundamental properties.

There are many surface modification techniques including mechanical treatment, thermal spraying, sol–gel processing, chemical and electrochemical treatments, and laser texturing [20–23]. To date, many studies have demonstrated the feasibility of generating hydrophilic or hydrophobic characteristics on coarse-grained metals by laser surface machining [24,25]. However, very little research has been conducted to examine the effect of laser surface modification on ultrafine-grained materials. Specifically, no studies are available describing the potential for modifying the surface properties of ultrafine-grained Ti to not only improve its hydrophobic or hydrophilic properties but also to retain a high mechanical strength. Accordingly, the present study was initiated to investigate the effect of applying a combination of HPT processing and a laser surface texturing method in order to improve the mechanical properties of CP-Ti and to control the hydrophilic and hydrophobic behavior in HPT samples for further research.

2. Experimental material and procedures

A grade 2 CP-Ti was purchased in the form of a round bar with a diameter of 12.7 mm from Titanium Industries UK, Ltd. (Birmingham, UK). The chemical composition in the grade 2 CP-Ti followed the ASTM B348-09 specification with a chemical requirement of maximum values of C of 0.08, O of 0.25, N of 0.03, H of 0.015 and Fe of 0.30 in weight percentage. The as-received material was annealed at 973 K for 2 h in a vacuum furnace to obtain a microstructure with an average grain size of ~65 μm and this is henceforth designated the as-annealed state. The rod was machined to a diameter of 10 mm and then cut into discs with thicknesses of ~0.8 mm [26]. These discs were processed to 1, 10 and 20 turns by HPT at room temperature under an imposed pressure of 6.0 GPa and with a rotational speed of 1 rpm. The processing was conducted using quasi-constrained conditions where there is a small outflow of material around the periphery of the disc during the torsional straining [27,28].

The effects of the number of turns on the microstructure and mechanical properties were investigated by observations using optical microscopy and transmission electron microscopy and by Vickers microhardness testing, respectively. The microstructures of the as-annealed samples were examined using an Olympus BH optical microscope (OM) at low magnification. The deformation microstructures after 10 and 20 turns of HPT processing were characterised using a JEOL1200 transmission electron microscope (TEM) operating under an accelerating voltage of 120 kV. TEM studies were conducted on standard 3 mm discs and the positions of the thin regions for high magnification observations were always located about 4 mm from the centres of the HPT-processed discs. The grain sizes were measured using the linear intercept method with image J with at least 300 grains measured for each sample.

Samples processed through 10 turns were subjected to short-term annealing for 10 min at temperatures of 473, 673, 873 and 973 K, respectively. In addition, the mechanical strengths of these 10 turn samples were evaluated in the HPT-processed condition and after post-HPT short-term annealing. The microhardness was measured using a hardness tester equipped with a Vickers indenter (FM300, Future-tech Corp.) under a load of 200 gf and with a dwell time of 15 s. Two dog-bone shaped miniature tensile specimens were cut from the 10 mm discs, with the gauges of the two tensile

specimens positioned symmetrically at 2 mm from the disc centres. The miniature tensile specimen had a gauge length of 1.0 mm, width of 1.0 mm and thickness of 0.6 mm. Tensile tests were carried out using a Zwick 30 KN Proline testing machine at room temperature (RT) operating at a constant rate of cross-head displacement with an initial strain rate of 1.0×10^{-3} s^{-1}.

To examine the effect of any surface modification, the samples processed by HPT to 1, 10 and 20 turns (without post-HPT short-term annealing) were processed by laser surface texturing using various laser powers, scanning speeds and holding times in order to evaluate the influence on the surface roughness and hydrophilic/hydrophobic properties. Prior to the laser surface texturing, the HPT-processed discs were ground with abrasive papers to similar roughnesses of ~560 ± 60 Å. These discs in the HPT-processed condition were then surface treated using a near-infrared laser (SPI G3) with a wavelength of 1064 nm, a repetition rate of 25 kHz, and a pulse duration of >10 ns. The texturing process was carried out using various laser powers in the range of 0.9–5.0 W and with scanning speeds in the range of 10–150 mm s^{-1}. The diameter of the laser spot, D_0, on the sample surface was calculated using the relationship

$$D_0 = 1.22 \times \left(\frac{\lambda \times F}{n \times W_d} \right) \times M^2 \tag{1}$$

where λ is the laser wavelength, F is the focal length, n is the refractive index, W_d is the nominal diameter of the laser beam and M^2 is the laser-quality factor. Equation (1) shows that the diameter of the laser beam is directly proportional to both the wavelength and the focal length. To increase the resolution of the texture pattern on the sample surface, the experimental setup was adjusted to reduce the laser spot size to ~40 μm.

The roughnesses of the laser-treated samples were measured using an Alpha step profiler (D-300, KLA) with a scanning speed of 0.4 mm s^{-1}, a scan line length of 5 mm and a load of 10 mg. The surface morphologies of the various samples were examined using an optical microscope (HRM-300, Huvitz). The hydrophilic/hydrophobic properties of the surface textured samples were investigated by measuring the contact angles of droplets of de-ionized water with volumes of 1 μL placed on the sample surface at a rate of 1 μL s^{-1}. The contact angle was measured three times and the average value was used for comparison purposes. The laser-treated surfaces were observed over a period from 1 to 13 days in order to fully evaluate the evolution of the surface hydrophilic or hydrophobic characteristics. New droplets were put on the laser-treated surface every day over the period from 1 to 13 days and the contact angle of each new droplet was then measured.

3. Experimental results

3.1. Microstructure and mechanical properties of the HPT-processed samples

Fig. 1 shows the microstructures of the HPT-processed samples after (a) 10 and (b) 20 turns. The grain size of the as-annealed sample was measured as about 65 μm but, as shown in Fig. 1, it was reduced significantly following HPT processing to approximately 70 nm for the 10 turns sample and 60 nm for the 20 turns sample. These similarities between the samples processed through 10 and 20 turns show that the discs are approaching a saturation condition where there is no significant further reduction in grain size [29].

The variations of the microhardness along the diameters of the 10 and 20 turns samples are shown in Fig. 2 where the lower dashed line at a microhardness of ~157 Hv denotes the hardness in
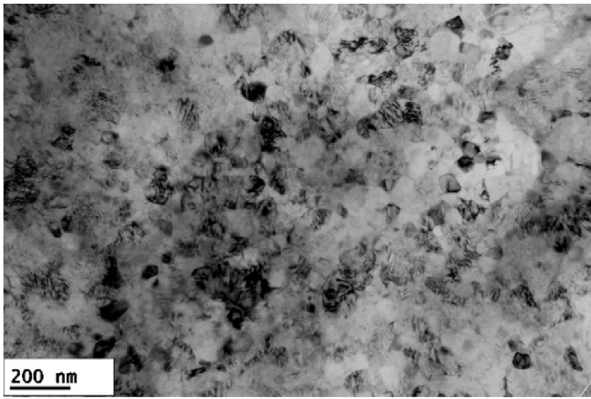
(a)
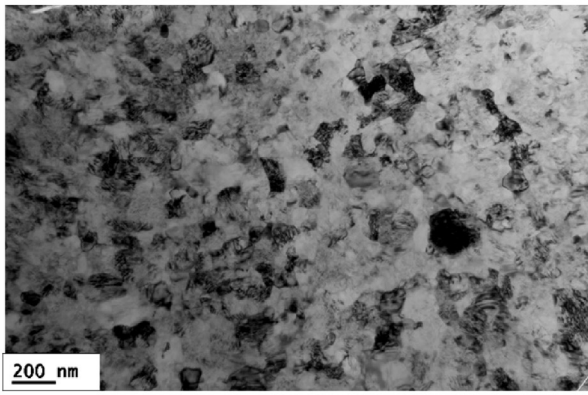
(b)

Fig. 1. Microstructures of samples processed by HPT to (a) 10 turns, (b) 20 turns from TEM observations.

the initial annealed condition. For the 10 and 20 turns samples, the hardness remains reasonably constant in the radial direction but with slightly lower values in the central region. It is apparent that the microhardness values increase with an increasing number of HPT turns and the highest hardness of up to ~350 Hv is obtained in
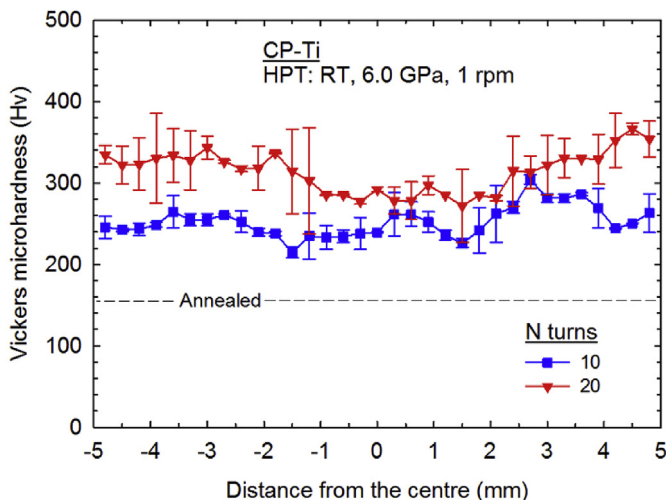
the sample processed through 20 turns.

The hardness and the grain size variations are plotted in Fig. 3 for the samples processed through 10 turns and then subjected to short-term annealing at 473, 673, 873 and 973 K. Thus, as the post-HPT short-term annealing temperature increases, the grain microstructure becomes less refined so that the measured average grain sizes increase from ~70 nm after HPT processing without annealing to ~1.9, ~3.1, ~3.9 and ~9.7 μm following anneals for 10 min at 473, 673, 873 and 973 K respectively. Concurrently, the hardness values drop as the post-HPT short-term annealing temperature increases. Therefore, as anticipated, the hardness decreases with increasing grain size.

Fig. 4 shows the engineering stress-engineering strain curves for the sample after 10 turns of HPT processing and for samples processed through 10 turns and then given short-term anneals for 10 min at temperatures of 473, 673, 873 and 973 K, respectively. The HPT-processed 10 turns sample has a very high strength but relatively low ductility as shown by the curve on the left in Fig. 4, such that failure occurs at approximately 840 MPa before the occurrence of any extensive plastic deformation. The low ductility in the HPT-processed 10 turns sample is attributed to the high dislocation density introduced by the torsional straining [10,30,31] which tends to limit the strain hardening ability of the material. By applying short-term annealing of 10 min on the HPT-processed 10 turns sample at 473 K, the ductility of the sample is significantly improved but with some reduction in strength. Further increases in the short-term annealing temperatures to 673, 873 and 973 K lead to reductions in the tensile strength with increasing annealing temperature due to the advent of rapid grain growth. Close inspection shows that the elongations to failure exhibit no special relationship with the short-term annealing temperatures but this is due to the slight variations that are an inherent feature of the gauge thicknesses for these various samples cut directly from the HPT discs. Despite the lack of any significant correlation between elongation and annealing temperature, it is readily apparent that the elongations of the samples after short-term annealing show a very significant improvement compared with the HPT-processed condition in the absence of any annealing.

3.2. Surface properties of the HPT-processed samples after laser surface texturing

Fig. 5 shows the surface roughness properties of samples processed by HPT through 1, 10 and 20 turns using laser powers in the
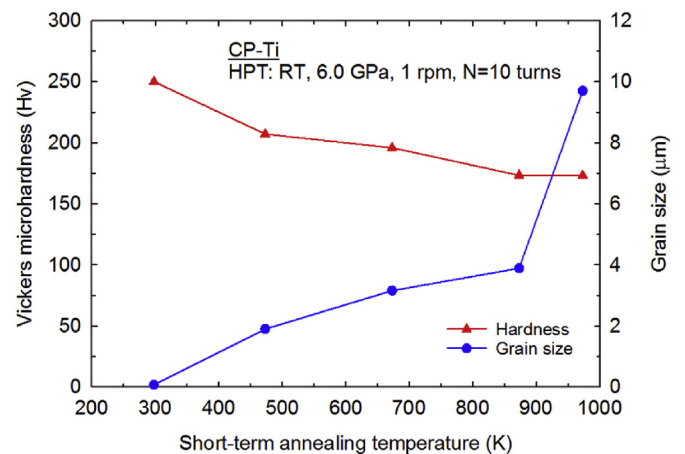

Fig. 2. Distribution of Vickers microhardness along diameters of HPT-processed discs.

Fig. 3. Hardness and grain size of samples in the conditions of 10 turns plus post-HPT short-term annealing at different temperatures.
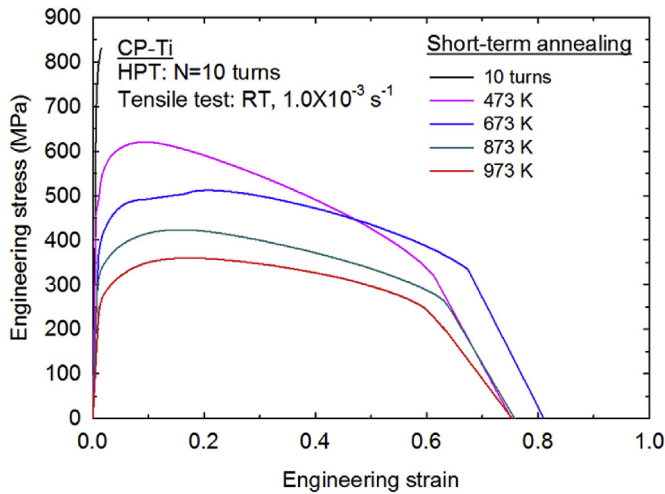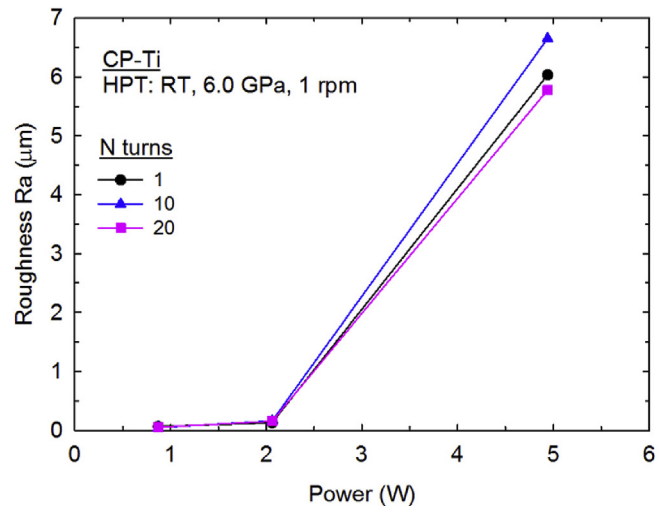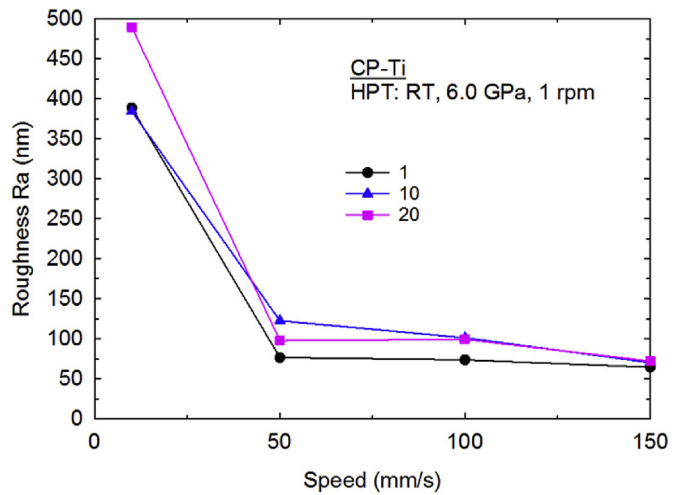
Fig. 4. Stress-strain curves from 10 turns sample and samples in the conditions of 10 turns plus post-HPT short-term annealing at different temperatures.

(a)

(b)

Fig. 5. Roughness of HPT samples after laser surface texture treatment under different conditions: (a) laser power and (b) laser scanning speed.

range of 0.9—5.0 W with a scanning speed of 150 mm s^{-1} in Fig. 5(a) and laser speeds in the range of 10—100 mm s^{-1} with a laser power of 2 W in Fig. 5(b). It is apparent from inspection of Fig. 5(a) that the roughness increases with increasing laser power for all HPT samples. For example, the roughness of the 20 turns sample increases from approximately 55 nm to 5.8 μm as the laser power is increased from 2.0 to 5.0 W. By contrast, and as displayed in Fig. 5(b), for a fixed laser power the roughness decreases with increasing scanning speed, where this reduction occurs especially at scanning speeds in the range of 10—50 mm s^{-1}.

Each contact angle is the average of three readings and the error range is ±5°. The value of the contact angle of the surface of the HPT-processed sample before laser texturing was 60°. Fig. 6 displays the variation of the contact angle with (a) the laser power and (b) the laser scanning speed. It is apparent from Fig. 6(a) that for samples processed by HPT through 1, 10 and 20 turns the contact angle decreases with increasing laser power, thereby demonstrating that samples become increasingly hydrophilic. This is directly consistent with the surface roughness variation shown in Fig. 5(a). From inspection of Fig. 6(a), the minimum contact angle, and therefore the greatest hydrophilicity, is found at approximately 20° for the HPT sample with 20 turns laser treated with a power of 5 W. By contrast, Fig. 6(b) shows the contact angle increases and therefore the samples become increasingly hydrophobic as the laser speed increases and this is probably due to the reduction in surface roughness as shown in Fig. 5(b). The contact angle of a drop of de-ionized water placed on an HPT-processed surface is reduced following the laser texture process. In addition, the contact angles on short-term annealed samples (N10 + 673 K short-term annealing) were also measured. Table 1 shows a comparison of results between HPT-processed samples and HPT + short-term annealed samples. With increasing laser power, the contact angle decreases for both conditions. The contact angle has similar variation tendencies with the different laser powers and therefore it is expected that short-term annealed samples have similar surface characteristics after laser surface treatment. Fig. 7 shows the variation of the contact angle with the observation period for up to 13 days for the 20 turns samples processed using a laser power of 5 W and a scanning speed of 150 mm s^{-1}. According to these results, and neglecting the scatter for short-term observation, the contact angle generally increases with increasing observation period. In Fig. 8 there are images for the 20 turns sample of the contact angle change a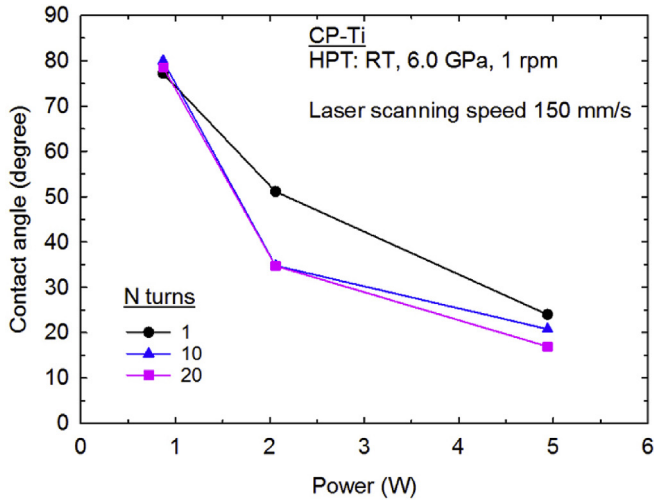fter (a) 1 day and (b) 13 days. Thus, noting that the maximum observation period in these experiments is 13 days, the contact angle of the 20 turns sample increases from 10° to 129°.
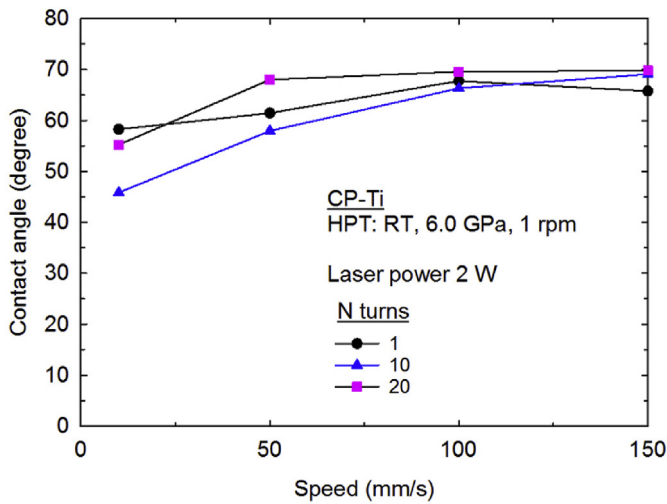
4. Discussion

The microstructure development in Fig. 1 demonstrates that HPT is very effective in producing grain refinement in the CP-Ti. The grain size before HPT processing was ~65 μm but after 10 and 20 turns of HPT processing the grain size was reduced to ~60—70 nm. By contrast, none of the conventional deformation procedures, such as forging, rolling or extrusion, provides the capability of achieving such a large extent of grain refinement. The hardness measurements on the HPT-processed samples in Fig. 2 show that there is a significant enhancement in the mechanical strength from the as-annealed value of ~157 Hv before HPT processing to a maximum value of ~350 Hv after HPT processing to 20 turns. There are reports of an α→ω phase transformation during HPT processing of CP-Ti

(a)

Fig. 7. Variation of contact angle of 20 turns samples with observation period.

(b)

Fig. 6. Contact angle of HPT samples after laser surface texture treatment under different conditions: (a) laser power and (b) laser scanning speed.

Table 1
A comparison of results for contact angle measurements between HPT-processed samples and HPT + short-term annealed samples.

Sample	(N10 + laser treatment) Contact angle	(N10 + 673 K annealing + laser treatment) Contact angle
Initial (No laser)	60 ± 5°	62.5 ± 5°
0.9 W	79.95°	68.45°
2 W	34.8°	46.25°
5 W	20.8°	23.35°

[32,33] and this may also make contributions to the material strength. X-ray analysis on the HPT-processed CP-Ti using the same batch as in the current research [26] confirmed the $\alpha \rightarrow \omega$ phase transformation during HPT processing. Thus, the HPT processing significantly refines the grain structure and enhances the mechanical strength, where the strength enhancement is attributed to the grain refinement, ω phase precipitation and high dislocation density.
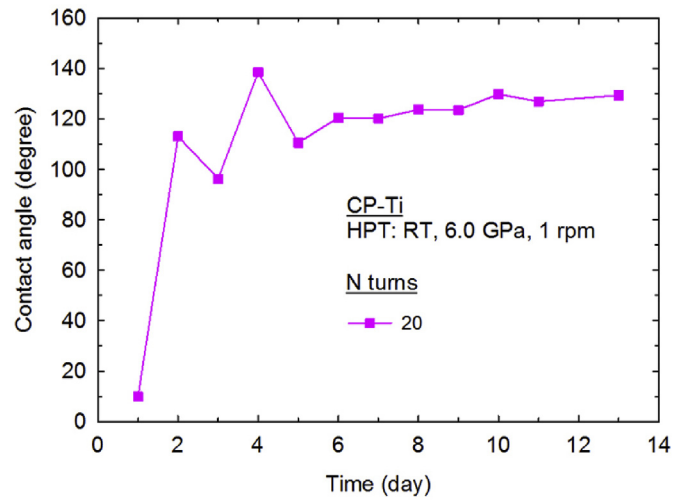
Nevertheless, although the HPT-processed material has high strength, the ductility is limited as shown by the curve for the 10 turns sample in Fig. 4. When materials are produced having ultrafine grain sizes, the strength is usually high but the ductility is low. This led to the well-established paradox of strength and ductility [34] which states explicitly that materials are either strong or they are ductile but not both. This paradox has received, and is continuing to receive, significant attention within the field of nanostructured materials [35]. A possible procedure to overcome this problem is to give the materials a short-term anneal immediately after processing. This technique was first introduced in early work on Ti [36,37] and more recently the same approach was used effectively on Al-1% Mg [38] and Ta [39].

In order to improve the ductility of HPT-processed materials, post-HPT short term annealing for 10 min was applied at selected temperatures from 473 to 973 K. Grain size measurements on post-HPT short-term annealed samples in Fig. 3 demonstrate that even at 473 K there is some grain growth after 10 min and when the short-term annealing temperature is further increased to 673 and 873 K the grain structures coarsen to ~3.1 and ~3.9 μm, respectively. With a further increase to 973 K the grain growth becomes significant and the average grain size is ~9.7 μm. This grain coarsening and significant grain growth correspond to a drop in the microhardness. The tensile testing results in Fig. 4 demonstrate that short-term annealed samples have much improved ductility but the strengths of the materials decrease with increasing short-term annealing temperatures due to the grain coarsening and, at the highest annealing temperature, to significant grain growth. It is suggested that a short-term annealing of 10 min at 473 K appears to represent the optimal short-term annealing condition producing a significant ductility improvement with only a concomitant limited drop in strength.

The surface roughness of the HPT-processed sample increases following either an increasing laser power or decreasing laser scanning speed as shown in Fig. 5. The roughness of the 20 turns sample increases from ~55 nm to ~5.8 μm as the laser power is increased from 1.0 to 5.0 W. Furthermore, the contact angle of the HPT-processed samples decreases with increasing laser power or decreasing laser scanning speed as shown in Fig. 6. Specifically, the contact angle of the HPT sample decreases from 76° to 20° with an increase in power from 1.0 to 5.0 W. This result shows that the HPT
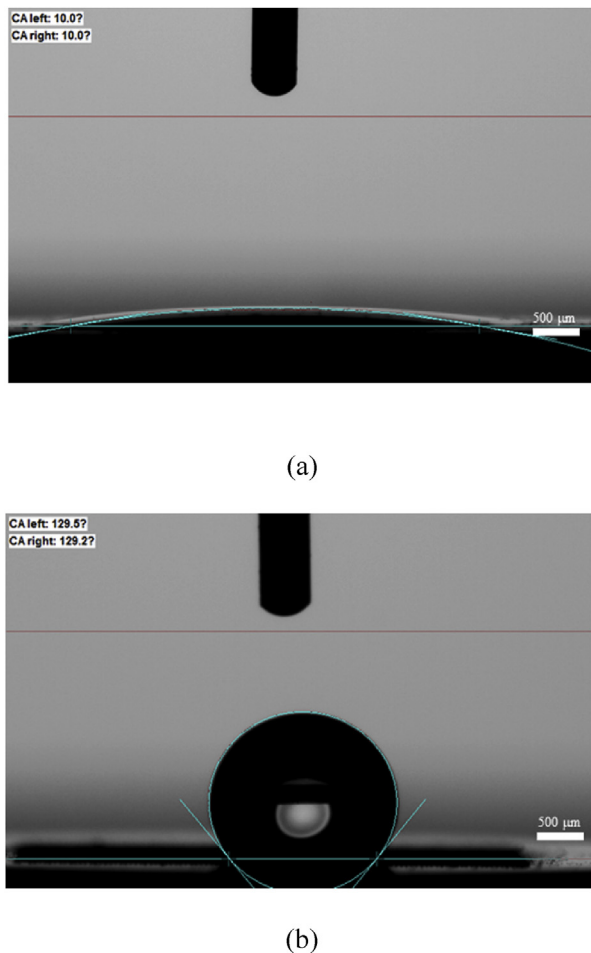
(a)

(b)

Fig. 8. Contact angle images for 20 turns samples with different observation periods: (a) 1 day, (b) 13 days.

sample has a hydrophilic surface after the laser surface treatment and thus provides a very good adhesion strength between the matrix and other media. By adjusting the observation period, the contact angle of the HPT-processed sample increases with increasing time as shown by the variation of the contact angle in Fig. 7. Thus, the contact angle of the 20 turns sample increases from 10° to 129° over an observation period of 13 days. It is readily apparent, therefore, that the HPT-processed sample has a hydrophilic surface due to the roughness induced immediately after the laser treatment. However, the surface feature transformed to a hydrophobic surface after 13 days storage probably due to the multi-scale roughness in the micro-scale and nano-scale that can absorb C atoms (C atom surface adsorption) and produce a surface transformation to a hydrophobic surface. A similar phenomenon, the Cassie—Baxter state [40], occurred due to the multi-scale texture formed mainly by the superimposed nano-scale and micro-scale ripples. Accordingly, after applying the laser surface texture treatments there should exist a desirable interface behavior in HPT-processed sample, the same as in the Cassie-Baxter state [40]. It is important to note also that after the laser treatment the texture surface has a thickness that is less than ~10 μm so that basically the bulk mechanical properties developed by HPT processing may be preserved.

Overall, the present results demonstrate, for the first time with HPT-processed samples, that the laser texture process leads to a roughening of the HPT-processed CP-Ti surface and hence it results

in a reduction in the contact angle. This means that the textured HPT samples have a hydrophilic property which is consistent with the predictions of the Wenzel model [41]. However, as the observation period increases so the contact angle also increases and this means that the surface changes from having a hydrophilic property to having a hydrophobic property. Previous studies showed that oxygen played an important role in the wettability transition process based on a wettability conversion mechanism. Thus, in other research on the Ti-6Al-4V alloy an EDX analysis revealed oxidation layer formation from day 2 to day 15 and this led to a 200% increase in the value of the contact angle [42] where a Cassie—Baxter state occurred due to the multi-scale texture formed mainly by superimposed nano-scale and micro-scale ripples. This produces an observed slight hydrophobic state [43] so that the storage process leads to the formation of a dual scale roughness structure as described in an earlier report [40,44].

A very recent report shows that a laser-ablated metallic surface exhibits an increase in the carbon content on the micro-burrs and the wettability change may be due to an increase in the amount of carbon [44]. However, there appeared to be no change in structure before and after the heat treatment and thus the increase in carbon content may be due to organic matter from the ambient air. Organic adsorption on the micro-burrs was proposed as an explanation for the wettability change and the presence of this −OH functional group on metal oxide films is well-known to be related to organic adsorption. This means that, after laser ablation, metal oxides with an −OH group can adsorb organic matter from the ambient air causing several weak hydrophobic groups (−CH3) to appear on the burrs. Thus, through no change in structure, an increase in carbon content and the appearance of strong hydrophobic groups, it follows that organic adsorption on the laser-ablated metallic micro-burrs was demonstrated. Therefore, the explanation for the time dependency of the surface wettability lies in the combined effects of surface morphology and surface chemistry. A preliminary XPS analysis on the laser-treated surface confirmed the content of the element C increased from 23.75 at% to 29.53 at.% for 4 and 40 days after laser treatment. It is reasonable to assume that the hydrophilic-to-hydrophobic transformation in the wetting behavior correlates directly with the amount of carbon that exists on the structured surface.

In summary, therefore, the present results on CP-Ti processed by HPT to produce an ultrafine-grained material provide a clear confirmation that laser surface texture processing can induce the hydrophilic-to-hydrophobic transformation. There is a potential for the control of the hydrophilic/hydrophobic properties by using a laser texturing treatment.

5. Summary and conclusions

1) HPT is effective in achieving significant grain refinement and strength enhancement in CP-Ti. Post-HPT short-term annealing improves the ductility of the material but there is a risk of introducing a strength drop at higher annealing temperatures.
2) The use of a post-HPT laser surface texturing process imbues the HPT-processed sample surface with a hydrophilic property as the result of a higher surface roughness. The hydrophilic tendency of the HPT-processed sample surface is enhanced with an increasing laser power but it is reduced with an increasing laser speed.
3) The contact angle increases with increasing observation period following the surface texturing process so that the surface of the CP-Ti changes from a hydrophilic behavior to a hydrophobic behavior as the observation period increases. The results show that laser surface texture processing can induce a hydrophilic-

to-hydrophobic transformation in the HPT-processed ultrafine grained CP-Ti.

Data availability

The raw/processed data required to reproduce these findings cannot be shared at this time as the data also forms part of an ongoing study.

Acknowledgements

References

[1] N. Eliaz, S. Shmueli, I. Shur, D. Benayahu, D. Aronov, G. Rosenman, The effect of surface treatment on the surface texture and contact angle of electrochemically deposited hydroxyapatite coating and on its interaction with bone-forming cells, Acta Biomater. 5 (2009) 3178–3191.

[2] Y. Li, C. Yang, H. Zhao, S. Qu, X. Li, Y. Li, New developments of Ti-based alloys for biomedical applications, Materials 7 (2014) 1709–1800.

[3] K. Subramani, W. Ahmed, P. Pachauri, Titanium nanotubes as carriers of osteogenic growth factors and antibacterial drugs for applications in dental implantology, in: Emerging Nanotechnologies in Dentistry, second ed., Elsevier, 2018, pp. 125–136.

[4] A.P. Zhilyaev, T.G. Langdon, Using high-pressure torsion for metal processing: fundamentals and applications, Prog. Mater. Sci. 53 (2008) 893–979.

[5] R.Z. Valiev, T.G. Langdon, Principles of equal-channel angular pressing as a processing tool for grain refinement, Prog. Mater. Sci. 51 (2006) 881–981.

[6] H. Shahmir, J. He, Z. Lu, M. Kawasaki, T.G. Langdon, Effect of annealing on mechanical properties of a nanocrystalline CoCrFeNiMn high-entropy alloy processed by high-pressure torsion, Mater. Sci. Eng., A 676 (2016) 294–303.

[7] V.V. Stolyarov, Y.T. Zhu, I.V. Alexandrov, T.C. Lowe, R.Z. Valiev, Influence of ECAP routes on the microstructure and properties of pure Ti, Mater. Sci. Eng., A 299 (2001) 59–67.

[8] V.V. Stolyarov, Y.T. Zhu, T.C. Lowe, R.Z. Valiev, Microstructures and properties of ultrafine-grained pure titanium processed by equal-channel angular pressing and cold deformation, J. Nanosci. Nanotechnol. 1 (2001) 237–242.

[9] H. Lin, J. Huang, T. Langdon, Relationship between texture and low temperature superplasticity in an extruded AZ31 Mg alloy processed by ECAP, Mater. Sci. Eng., A 402 (2005) 250–257.

[10] A.P. Zhilyaev, G. Ringot, Y. Huang, J.M. Cabrera, T.G. Langdon, Mechanical behavior and microstructure properties of titanium powder consolidated by high-pressure torsion, Mater. Sci. Eng., A 688 (2017) 498–504.

[11] F. Niekiel, P. Schweizer, S.M. Kraschewski, B. Butz, E. Spiecker, The process of solid-state dewetting of Au thin films studied by in situ scanning transmission electron microscopy, Acta Mater. 90 (2015) 118–132.

[12] B. Luo, P.W. Shum, Z. Zhou, K. Li, Preparation of hydrophobic surface on steel by patterning using laser ablation process, Surf. Coat. Technol. 204 (2010) 1180–1185.

[13] M.H. Kwon, H.S. Shin, C.N. Chu, Fabrication of a super-hydrophobic surface on metal using laser ablation and electrodeposition, Appl. Surf. Sci. 288 (2014) 222–228.

[14] Y. Oh, M. Lee, Single-pulse transformation of Ag thin film into nanoparticles via laser-induced dewetting, Appl. Surf. Sci. 399 (2017) 555–564.

[15] O. Raimbault, S. Benayoun, K. Anselme, C. Mauclair, T. Bourgade, A.-M. Kietzig, P.-L. Girard-Lauriault, S. Valette, C. Donnet, The effects of femtosecond laser-textured Ti-6Al-4V on wettability and cell response, Mater. Sci. Eng. C 69 (2016) 311–320.

[16] T. Hong, K. Chi, H. Lin, Y. Wu, Laser surface modification for rapid oxide layer formation on Ti-6Al-4V, J. Laser Micro Nanoeng. 9 (2014) 64.

[17] N. Moritz, S. Areva, J. Wolke, T. Peltola, TF-XRD examination of surface-reactive TiO2 coatings produced by heat treatment and CO2 laser treatment, Biomaterials 26 (2005) 4460–4467.

[18] C.N. Elias, Y. Oshida, J.H. Lima, C.A. Muller, Relationship between surface properties (roughness, wettability and morphology) of titanium and dental

[19] L. Ponsonnet, K. Reybier, N. Jaffrezic, V. Comte, C. Lagneau, M. Lissac, C. Martelet, Relationship between surface properties (roughness, wettability) of titanium and titanium alloys and cell behaviour, Mater. Sci. Eng. C 23 (2003) 551–560.

[20] M. Apreutesei, A. Billard, P. Steyer, Crystallization and hardening of Zr-40 at.% Cu thin film metallic glass: effects of isothermal annealing, Mater. Des. 86 (2015) 555–563.

[21] A. Dunn, T.J. Wasley, J. Li, R.W. Kay, J. Stringer, P.J. Smith, E. Esenturk, C. Connaughton, J.D. Shephard, Laser textured superhydrophobic surfaces and their applications for homogeneous spot deposition, Appl. Surf. Sci. 365 (2016) 153–159.

[22] X. Liu, P.K. Chu, C. Ding, Surface modification of titanium, titanium alloys, and related materials for biomedical applications, Mater. Sci. Eng. R Rep. 47 (2004) 49–121.

[23] U. Zulfiqar, S.Z. Hussain, M. Awais, M.M.J. Khan, I. Hussain, S.W. Husain, T. Subhani, In-situ synthesis of bi-modal hydrophobic silica nanoparticles for oil-water separation, Colloid. Surface. A: Physiochem. Eng. Aspect 508 (2016) 301–308.

[24] J. Fu, Y. Zhu, C. Zheng, R. Liu, Z. Ji, Evaluate the effect of laser shock peening on plasticity of Zr-based bulk metallic glass, Optic Laser. Technol. 73 (2015) 94–100.

[25] B.S. Yilbas, H. Ali, Laser texturing of Hastelloy C276 alloy surface for improved hydrophobicity and friction coefficient, Optic Laser. Eng. 78 (2016) 140–147.

[26] Y. Huang, S. Mortier, P.H.R. Pereira, P. Bazarnik, M. Lewandowska, T.G. Langdon, Thermal stability and mechanical properties of HPT-processed CP-Ti, IOP Conf. Ser. Mater. Sci. Eng. 194 (2017), 012012.

[27] R.B. Figueiredo, P.R. Cetlin, T.G. Langdon, Using finite element modeling to examine the flow processes in quasi-constrained high-pressure torsion, Mater. Sci. Eng., A 528 (2011) 8198–8204.

[28] R.B. Figueiredo, P.H.R. Pereira, M.T.P. Aguilar, P.R. Cetlin, T.G. Langdon, Using finite element modeling to examine the temperature distribution in quasi-constrained high-pressure torsion, Acta Mater. 60 (2012) 3190–3198.

[29] S. Sabbaghianrad, T.G. Langdon, An evaluation of the saturation hardness in an ultrafine-grained aluminum 7075 alloy processed using different techniques, J. Mater. Sci. 50 (2015) 4357–4365.

[30] H. Shahmir, T.G. Langdon, Characteristics of the allotropic phase transformation in titanium processed by high-pressure torsion using different rotation speeds, Mater. Sci. Eng., A 667 (2016) 293–299.

[31] H.Y. Um, B.H. Park, D.H. Ahn, M.I. Abd El Aal, J. Park, H.S. Kim, Mechanical and biological behavior of ultrafine-grained Ti alloy aneurysm clip processed using high-pressure torsion, J. Mech. Behav. Biomed. Mater. 68 (2017) 203–209.

[32] A.R. Kilmametov, A.V. Khristoforov, G. Wilde, R.Z. Valiev, X-ray studies of nanostructured metals processed by severe plastic deformation, Z. Kristallogr. Suppl. (2007) 339–344.

[33] K. Edalati, E. Matsubara, Z. Horita, Processing pure Ti by high-pressure torsion in wide ranges of pressures and strain, Metall. Mater. Trans. 40 (2009) 2079–2086.

[34] R. Valiev, I. Alexandrov, Y. Zhu, T. Lowe, Paradox of strength and ductility in metals processed by severe plastic deformation, J. Mater. Res. 17 (2002) 5–8.

[35] P. Kumar, M. Kawasaki, T.G. Langdon, Review: overcoming the paradox of strength and ductility in ultrafine-grained materials at low temperatures, J. Mater. Sci. 51 (2016) 7–18.

[36] A. Sergueeva, V. Stolyarov, R. Valiev, A. Mukherjee, Advanced mechanical properties of pure titanium with ultrafine grained structure, Scripta Mater. 45 (2001) 747–752.

[37] R. Valiev, The effect of annealing on tensile deformation behavior of nano-structured SPD titanium, Scripta Mater. 49 (2003) 669–674.

[38] O. Andreau, J. Gubicza, N.X. Zhang, Y. Huang, P. Jenei, T.G. Langdon, Effect of short-term annealing on the microstructures and flow properties of an Al–1% Mg alloy processed by high-pressure torsion, Mater. Sci. Eng., A 615 (2014) 231–239.

[39] N. Maury, N.X. Zhang, Y. Huang, A.P. Zhilyaev, T.G. Langdon, A critical examination of pure tantalum processed by high-pressure torsion, Mater. Sci. Eng., A 638 (2015) 174–182.

[40] A.M. Kietzig, S.G. Hatzikiriakos, P. Englezos, Patterned superhydrophobic metallic surfaces, Langmuir 25 (2009) 4821–4827.

[41] K.Y. Yeh, L.J. Chen, J.Y. Chang, Contact angle hysteresis on regular pillar-like hydrophobic surfaces, Langmuir 24 (2008) 245–251.

[42] P. Bizi-bandoki, S. Valette, E. Audouard, S. Benayoun, Time dependency of the hydrophilicity and hydrophobicity of metallic alloys subjected to femtosecond laser irradiations, Appl. Surf. Sci. 273 (2013) 399–407.

[43] D.S. Patel, A. Singh, K. Balani, J. Ramkumar, Topographical effects of laser surface texturing on various time-dependent wetting regimes in Ti6Al4V, Surf. Coat. Technol. 349 (2018) 816–829.

[44] C.V. Ngo, D.M. Chun, Control of laser-ablated aluminum surface wettability to superhydrophobic or superhydrophilic through simple heat treatment or water boiling post-processing, Appl. Surf. Sci. 435 (2018) 974–982.